In Situ Luminescence Measurement from Silica Glasses Irradiated with 20 keV H^- Ions

Ying-Jie Chu(褚莹洁)[1], Guang-Fu Wang(王广甫)[1,2**], Meng-Lin Qiu(仇猛淋)[1], Mi Xu(胥密)[1], Li Zheng(郑力)[1]

[1]*College of Nuclear Science and Technology, Beijing Normal University, Beijing 100875*
[2]*Beijing Radiation Centre, Beijing 100875*

(Received 5 July 2016)

A new low-energy negative-ion induced luminescence setup was recently developed at the injector of the GIC4117 $2 \times 1.7\,MV$ Tandem accelerator in Beijing Normal University. In situ luminescence measurements are performed on silica glass by using 20 keV H^- ions at room temperature. Gauss fitting of the spectra revealed six overlapping components at about 2.7 eV, 2.4 eV, 1.9 eV, 1.8 eV, 4.2 eV, and 3.6 eV, which except for the new observed emission band at 3.6 eV are assigned to the creation of type Ⅱ oxygen-deficient centers, E′ centers, non-bridging oxygen hole centers with different precursor states, and type-I oxygen-deficient centers. The fitted results of the saturation concentration show that self-trapped exciton recombination at type-Ⅱ oxygen-deficient centers is the main luminescence emission process. The evolution of the luminescence intensity and full width at half maximums as a function of ion fluence is also discussed. It is found that the number of recombination centers reaches its maximum at lower fluence, and the area ratio between blue bands and red bands is much lower than that under high energy H^+ ion irradiation.

PACS: 61.82.Ms, 61.80.Jh, 42.70.Ce DOI: 10.1088/0256-307X/33/10/106101

Ion-beam-induced luminescence (IBIL) is a very sensitive technique for identifying impurities and structural changes in insulators and semiconductors during ion irradiation.[1,2] The main advantages of the IBIL technique are its in situ measurement characteristics that do not require interruption of irradiation and avoid the influence of possible recovery effects. Moreover, this technique can be used to investigate defects even below the order of parts per million.[3,4] Additionally, different ion beam species and energies allow one to vary the depth of the material compared with other optical techniques (photoluminescence, cathodoluminescence, etc.).[5] This technique can be widely used in the field of physics, geology, and archaeology, as well as biology and chemistry.[1,4,5]

Most works focused on radiation damage in insulators have been performed with positive ions. Insulators are easily charged under irradiation of positive ions, and the charging voltage even increases to the value corresponding to the ion energy, which may lead to a localized electrical potential, deviated photon intensity scattering, and transformations between different forms of defects.[6–8] Therefore, the observed luminescence spectra are influenced by surface charging or other instabilities of the incident beam.[9] However, negative-ion bombardment has a particular 'charge-up free' feature. The charge of incoming negative ions is compensated for by that of outgoing secondary electrons.[10,11] Therefore, negative-ion irradiation makes it possible to suppress the surface voltage down to several volts. The luminescence induced by negative ions is thus considered to be charge-up free for studying the radiation damage of insulators such as silica glasses.

In this work, a new low-energy negative-ion induced luminescence setup was developed at the injector of the GIC4117 $2 \times 1.7\,MV$ Tandem accelerator (Beijing Normal University) based on the original negative-ion implantation system.[12] In situ measurements of luminescence from silica glass under 20 keV H^- ions irradiation were performed. Reliable spectra were obtained to investigate both the defects generation with associated emission processes and the damage evolution with fluence.

A schematic diagram of the experimental apparatus is given in Fig. 1. The setup can detect luminescence signals induced by negative ions with energies at or less than 20 keV. Negative ions were generated from the GIC860A Cs sputtering negative-ion source. Two 45° analyzing magnets were used to transport the selected ion beam to either a retractable Faraday cup for current measurement or a sample on the samples holder for ion irradiation. The vacuum was maintained below 3×10^{-6} torr during irradiation. The light emitted from samples was transmitted through a 600-μm diameter silica optical fiber. To achieve the optimal sensitivity, the optical fiber was inserted into the vacuum chamber through a vacuum feed-through, and its end was perpendicular to the sample surface and about 2 cm away from it. The ion induced luminescence was collected by a spectrometer (Ocean Optics QEPRO), with a resolution of 2 nm and band-

**Corresponding author. Email: 88088@bnu.edu.cn
© 2016 Chinese Physical Society and IOP Publishing Ltd

width of 200–1000 nm. A 100-μm entrance slit was employed to achieve high luminescence detection efficiency.

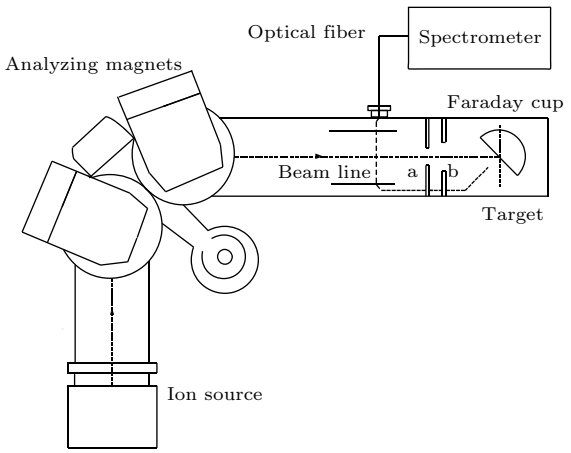

Fig. 1. Schematic diagram of the IBIL experimental configuration: (a) beam aperture, (b) suppressor electrode.

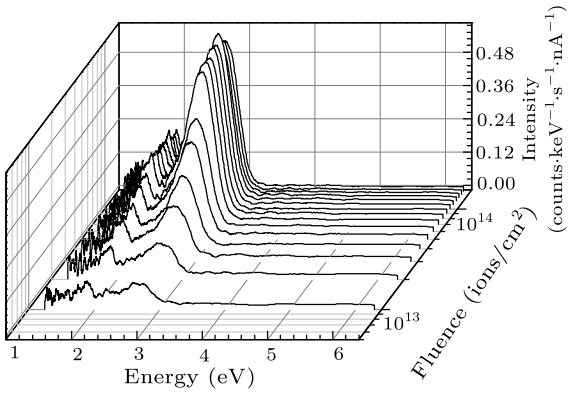

Fig. 2. Emission spectra for silica glass irradiated with 20 keV H^- at different fluences.

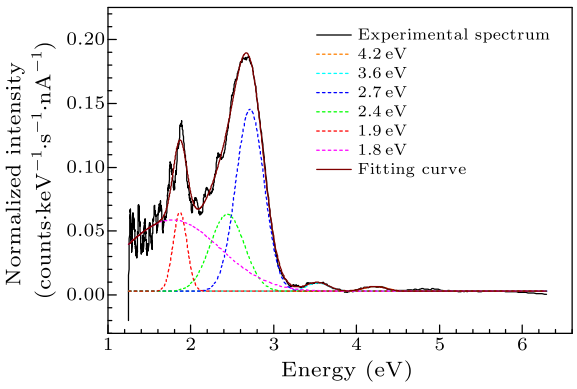

Fig. 3. Spectrum (solid line plots) induced by 20 keV H^- at a fluence of 5×10^{13} ions/cm^2. The dashed lines indicate deconvolution by Gaussian functions peaked at 4.2, 3.6, 2.7, 2.4, 1.9 and 1.8 eV.

Commercially available samples of two-sided polished silica glass with a size of $13 \times 13 \times 1$ mm^3 (JCK02, OH content: 1100 ppm) produced by the China Building Materials Academy were used. The concentration of metal impurities is less than 2 ppm and no apparent luminescence peaks associated with metallic impurities in the above samples were detected in our IBIL experiment. In this study, a 20 keV H^- beam, with current of 580 nA and a diameter of 8 mm, was incident on the sample at 45° to the surface normal at room temperature. An integration time of 3 s was selected for the luminescence spectra. The ion fluence was determined by direct current integration from the target.

The stopping power of 20 keV protons in silica glass was calculated with the SRIM code. The electronic stopping power is about 9×10^{-2} keV/nm, lower than the material dependent threshold stopping power for the production of cylindrical ion tracks.[13] The magnitude of the nuclear energy loss is around 7×10^{-4} keV/nm.

Figure 2 shows the observed ion-induced luminescence spectra of the silica glass induced by 20 keV H^- at fluences ranging from 3.21×10^{13} ions/cm^2 to 9.64×10^{14} ions/cm^2. To avoid errors in peak positions and incorrect numbers of component peaks, the spectra have been converted from wavelength (λ) signals of $I(\lambda)d\lambda$ versus λ to an energy scale of $I(E)dE$ versus E.[14] It is found that the luminescence intensity initially rises with the fluence and then slowly decreases to a saturation level at higher fluences.

Two broad emission bands are observed, including one peak at around 1.9 eV, and the other in the blue spectrum region around 2.4–2.7 eV. Six overlapping components centered at about 4.2 eV, 3.6 eV, 2.7 eV, 2.4 eV, 1.9 eV and 1.8 eV are derived from a Gauss fitting function, as shown in Fig. 3.

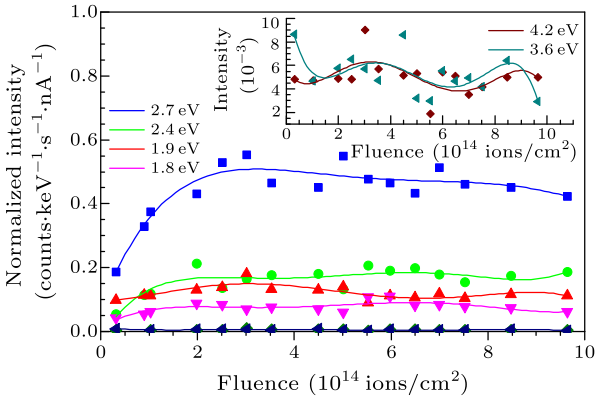

Fig. 4. Evolution of emission bands around 4.2, 3.6, 2.7, 2.4, 1.9 and 1.8 eV with H^- fluence. The solid lines are the results fitted by a polynomial. The inset shows the intensities at 3.6 eV and 4.2 eV.

The intensity of each Gaussian component, plotted as a function of H^- fluence, is presented in Fig. 4. Emission bands around 4.2 eV and 3.6 eV show a much smaller intensity compared with the other bands, as shown at the top inset of Fig. 4. The luminescence intensity fluctuates and remains almost constant with fluence. The 4.2 eV peak was ascribed to the diamag-

netic neutral relaxed oxygen vacancy, which is known as a type-I oxygen deficient (ODC I).[8] The origin of the 3.6 eV band was not reported earlier. However, the intensity of the two bands showed a similar trend with the fluence, which was clear at the early stage of irradiation. Therefore, the 3.6 eV band may have a related origin with oxygen deficient defects. The intensity of the 2.7 eV band first increased to the maximum at a fluence around 3×10^{14} ions/cm^2 and slowly decreased to a saturation level. The 2.7 eV band is generally attributed to a type II oxygen-deficient centers (ODC II) related to the Frenkel process.[15] The 2.3–2.4 eV peak is observed due to the radiative recombination of STEs associated with E′ centers in amorphous silica.[8] The red bands at 1.9 eV and 1.8 eV can be regarded as a probe for the on-going generation of NBOHCs with different precursor states, the breaking of the Si–OH groups and the Si–O–Si bonds dissociation.[8,16]

All of the above emission bands except that at 3.6 eV have been found to be very similar to spectra induced by MeV H^+ ions in spite of small differences in peak positions and widths, considering the instrumental factors and Gaussian fitting deviations,[3,4,17] where the projected range could reach tens of μm in silica glass, and the signal is mainly from the bulk recombination centers. However, the ion range and its straggle are 183 nm and 60 nm using 20 keV protons simulated by TRIM. This means that the luminescence observed in this work may be influenced much more by surface defects than by radiation of high energy ions. As a result of the interaction with atomic H at room temperature, some of the ODC II were converted to nonluminescent centers H(I).[16] The broken bonds in the surface adsorb H^+ from ambient air or OH breaking, thus NBOHCs are transformed into ≡Si–OH. In addition, defects clustering and Si precipitation also account for the intensity reduction shown by the x-ray absorption fine structure (XAFS).[18]

The light emission under irradiation results from the recombination of electron–hole pairs at recombination defect centers associated with radiation damage. The luminescence yield $Y(\Phi)$ of a certain band is assumed to be proportional to the irradiation fluence Φ, incident ion energy E, and the concentration of the luminescent centers (fluence dependent) $N(\Phi)$. Therefore, $Y(\Phi)/\Phi E$ can be used to compare the number of recombination centers for emission bands.[4,19] The competition between the generation and recombination processes of STEs will lead to a steady population under continuous irradiation. The number of STEs can roughly be taken as a constant,[20] and the evolution for the concentration of the luminescent centers per unit area shows the Poisson-type behavior,[21]

$$N = N_{\rm s}(1-\exp(-\sigma\phi)), \tag{1}$$

where $N_{\rm s}$ is the saturation concentration, and σ is the effective production cross section. The values of $N_{\rm s}$ deduced from the normalized luminescence yield in our IBIL measurements are 0.20, 0.09, 0.03 and 0.07 cm^{-2} for ODCII, E′ centers and NBOHC with different precursor states, respectively. The corresponding σ of defects are 1.58, 0.96, 2.15 and 1.68 cm^2, respectively. The concentration of ODC II is much higher than that of E′ and NBOHC, indicating that the Frenkel pair is the main luminescence generation process. The efficiency of the Frenkel process is influenced by the number of strained Si–O–Si bonds,[15] thus the increased creation of oxygen vacancies indicates that the concentration of strained Si–O–Si bonds is changed during irradiation.

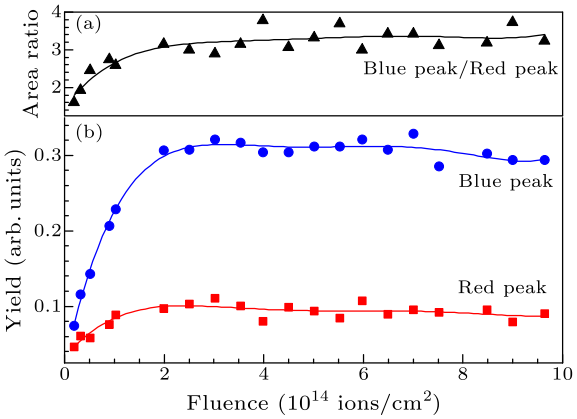

Fig. 5. Yield of blue bands (2.4–2.7 eV) and red bands (1.8–1.9 eV) and the area ratio between two peaks, plotted as a function of ion fluence. The solid lines are fitted polynomials.

Another piece of information is the evolution of the yield and its ratio between two broad peaks with fluences under 20 keV H^- irradiation, as given in Fig. 5. The luminescence yield of blue (2.4–2.7 eV) and red (1.8–1.9 eV) bands first increases to a maximum with H^- fluence $\phi_{\rm M}$ and gradually decreases to saturation after prolonged irradiation, which is similar to the results reported in the previous work,[3,4,17,18] while it was noted that $\phi_{\rm M}$ around 3×10^{14} ions/cm^2 and 2×10^{14} ions/cm^2 is much lower than the results in the above-mentioned studies, which were performed with H^+ ions at different energies. The ratio can give information on the relative concentration of respective recombination centers. The growth rate of the red band is clearly smaller than that of the blue band, which is in agreement with the results obtained by MeV H^+ ions.[4] However, the area ratio between blue bands and red bands is much lower compared with irradiation of high-energy H^+ ions. It is interesting that the local concentration of Si–OH impurities near the surface of the samples could be higher than that in the bulk.[22] This could be explained by the fact that the broken bonds of high-OH silica glass tend to trap more hydrogen than low-OH silica glass in the form of Si–

OH or Si–H bonds. Therefore, the red band emissions were enhanced during irradiation.

It is worth noting that Yoshida *et al.*[18] and Nagata *et al.*[23] reported that the peak position and full width at half maximums (FWHMs) of luminescence spectra were influenced at higher fluences under 10–20 keV H^+ ion irradiation. Figure 6 gives the evolution of the FWHM for 2.7, 2.4, 1.9 and 1.8 eV bands with H^- fluence. Fluctuations were also observed among these four emission bands, suggesting multiple origins of the luminescence centers. Alternative color centers could be generated which emit luminescence in the energy region near these four emission bands. This means that the recombination of defects with different precursor states could show similar measured peak energies. It could also be explained by the theory of approximate energy levels which shows one certain color center emits light with small differences in peak width due to the splitting of the energy level. However, it is observed that the FWHMs of the spectra did not change during 0.1–2 MeV H^+ radiation,[23] thus FWHM changes may be related to the surface effects, which will need to be further confirmed in future studies.

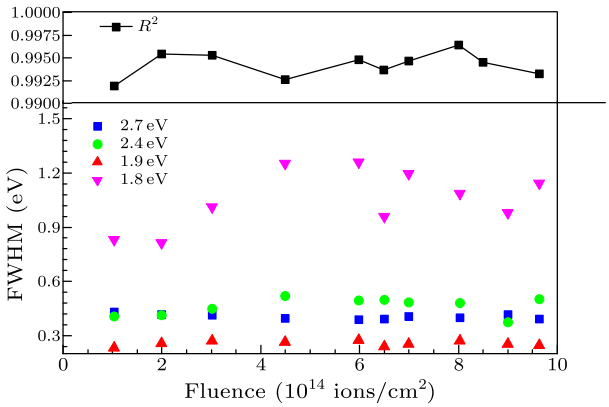

Fig. 6. FWHM changes of four emission bands at around 2.7, 2.4, 1.9 and 1.8 eV as a function of the H^- fluence. Correlation coefficient (R^2) is shown at the top inset.

In conclusion, in situ luminescence measurements of silica glass irradiated with 20 keV H^- ions have been performed at the injector of the GIC4117 Tandem accelerator. Four emission bands peaked around 1.9 eV, 2.4–2.7 eV, 3.6 eV and 4.2 eV are observed, and their origins are explained in the literature, except for the new luminescence bands at 3.6 eV. The saturation concentration obtained in this work shows that the STE recombination at ODC Ⅱ centers is the main luminescence emission process. Both the luminescence yields and yield ratio of the blue and red bands increase with fluence initially, and the yield reaches a maximum at about $2–3 \times 10^{14}$ ions/cm^2, which is much lower than the reported results obtained with H^+ ion irradiation at different energies, and then decreases slowly. The evolution of the luminescence intensity and FWHM as a function of ion fluence could be explained by the creation, transformation and clustering of defects.

References

[1] Townsend P D, Khanlary M and Hole D E 2007 *Surf. Coat. Technol.* **201** 8160
[2] Townsend P D and Crespillo M L 2015 *Phys. Procedia* **66** 345
[3] Bachiller-Perea D, Jiménez-Rey D, Muñoz-Martín A et al 2015 *J. Non-Cryst. Solids* **428** 36
[4] Crespillo M L, Graham J T, Zhang Y et al 2016 *J. Lumin.* **172** 208
[5] Townsend P D and Wang Y F 2013 *Energy Procedia* **41** 64
[6] Crespillo M L, Graham J T, Zhang Y et al 2016 *Rev. Sci. Instrum.* **87** 24902
[7] Tanabe T, Fujiwara M, Iida T et al 1995 *Fusion Eng. Des.* **29** 435
[8] Stevens-Kalceff M A 2009 *Mineral. Mag.* **73** 585
[9] Tanabe T, Fujiwara M and Miyazaki K 1996 *J. Nucl. Mater.* **233** 1344
[10] Tsuji H, Gotoh Y and Ishikawa J 1998 *Nucl. Instrum. Methods Phys. Res. Sect.* B **141** 645
[11] Ishikawa J 2007 *Nucl. Instrum. Methods Phys. Res. Sect.* B **261** 1032
[12] Zheng C, Wang G, Chu Y et al 2016 *Nucl. Instrum. Methods Phys. Res. Sect.* B **370** 73
[13] Agulló-López F, Climent-Font A, Muñoz-Martín A et al 2016 *Prog. Mater. Sci.* **76** 1
[14] Wang Y and Townsend P D 2013 *J. Lumin.* **142** 202
[15] Kajihara K, Hirano M, Skuja L et al 2008 *Phys. Rev.* B **78** 094201
[16] Skuja L 1998 *J. Non-Cryst. Solids* **239** 16
[17] Nagata S, Yamamoto S, Inouye A et al 2007 *J. Nucl. Mater.* **367** 1009
[18] Yoshida T, Tanabe T, Watanabe M et al 2004 *J. Nucl. Mater.* **329** 982
[19] Peña-Rodríguez O, Jiménez-Rey D, Manzano-Santamaría J et al 2012 *Appl. Phys. Express* **5** 011101
[20] Bachiller-Perea D, Jiménez-Rey D, Muñoz-Martín A et al 2016 *J. Phys.* D **49** 088501
[21] Ma M, Chen X, Yang K et al 2010 *Nucl. Instrum. Methods Phys. Res. Sect.* B **268** 67
[22] Messina F, Vaccaro L and Cannas M 2010 *Phys. Rev.* B **81** 035212
[23] Nagata S, Katsui H, Tsuchiya B et al 2009 *J. Nucl. Mater.* **386** 104